AN ADMM ALGORITHM FOR PEAK TRANSMISSION ENERGY MINIMIZATION IN SYMBOL-LEVEL PRECODING

Yatao Liu, Mingjie Shao and Wing-Kin Ma

Department of Electronic Engineering, The Chinese University of Hong Kong, Hong Kong SAR, China
E-mail: {ytliu, mjshao, wkma}@ee.cuhk.edu.hk

ABSTRACT

This paper considers symbol-level precoding (SLP) for the multiuser multiple-input single-output (MISO) downlink scenario. By exploiting symbol constellation information, SLP has the ability to achieve much better performance than traditional linear beamforming schemes. In this work, we propose an SLP design formulation under quadrature amplitude modulation (QAM) constellations. The objective of the design is to minimize the peak transmission energy over symbol time slots, while, at the same time, satisfying pre-specified symbol error probability (SEP) requirements of all the users. This kind of design can reduce the energy spread over symbol time. The resulting problem is a large-scale convex problem, and we develop an efficient alternating direction method of multipliers (ADMM) algorithm for the problem. Simulation results demonstrate that our proposed algorithm significantly outperforms some conventional linear beamforming schemes.

***Index Terms*—** multiuser MISO, symbol-level precoding, peak transmission energy, ADMM.

1. INTRODUCTION

In the multiuser multiple-input single-output (MISO) downlink scenario, linear beamforming has been shown to be effective in improving performance such as energy efficiency and the total throughput [1–6]. The rationale of linear beamforming is to suppress the multiuser interference by exploiting channel state information (CSI). In such study, interference is often treated as harmful signals. In the early 2010, a novel type of nonlinear precoding schemes, called constructive interference, directional modulation or symbol-level precoding (SLP), was proposed. SLP suggests that by exploiting the symbol constellation information, interference can be actually made use of to improve system performance. Numerous studies have shown that SLP can provide significant performance gains compared with linear beamforming schemes.

The initial idea of SLP was proposed in [7–9], where interference is manipulated at the base station (BS) to push received signals deeper into the correct detection region. A number of subsequent research, which uses convex optimization-based SLP designs, appeared later [10–16]. In those studies, SLP was designed to satisfy certain signal-to-noise ratio (SNR) requirements. The form of SNR is dependent on the symbol constellation structure, and the SNR expressions are totally different for quadrature amplitude modulation (QAM) and M-ary phase shift keying (PSK) constellations. Recently the idea of SLP has been extended to many other scenarios, such as physical-layer security [17], large-scale antenna selection [18], energy harvesting [19] and robust precoding designs [20].

In this paper, we consider a symbol error probability (SEP)-constrained SLP design under QAM constellations. The goal is to minimize the peak energy of the transmit signals over symbol time. By minimizing the peak energy, we try to reduce the transmission energy in the instantaneous sense, not in the average sense. This kind of design is helpful in reducing the energy spread over symbol time. Our SEP-constrained SLP design is formulated as a large-scale non-smooth convex optimization problem (as will be described, this is because our design also optimizes the QAM constellation ranges across symbol time, which can lead to considerable improved performance). As the main contribution of this paper, we propose an alternating direction method of multipliers (ADMM) algorithm to solve the problem efficiently. By applying the ADMM algorithm, the resulting large-scale problem is decoupled into per-time-slot problems, which allows us to solve them in a distributed manner. Simulation results demonstrate that our design outperforms traditional linear beamforming in terms of peak transmission energy.

It should be mentioned that the formulation of the considered SEP-constrained SLP design was derived in our previous work [21]; that work also unveils a hidden equivalence relation between SLP and zero-forcing (ZF) beamforming. However, efficient optimization schemes for the design were not studied in [21].

2. SYSTEM MODEL AND PROBLEM FORMULATION

The scenario we consider is as follows. A BS, equipped with N antennas, tries to transmit K independent symbol streams to K single-antenna users in a simultaneous and unicast fashion. The channels from the BS to the users are assumed to be frequency-flat block faded channels. The received signals of all users over one transmission block is modeled as

$$y_{i,t} = \boldsymbol{h}_i^H \boldsymbol{x}_t + v_{i,t}, \quad i = 1, \ldots, K, \quad t = 1, \ldots, T, \qquad (1)$$

where $y_{i,t} \in \mathbb{C}$ is the received signal of user i at symbol time t; $\boldsymbol{x}_t \in \mathbb{C}^N$ is the transmitted signal at symbol time t; $\boldsymbol{h}_i \in \mathbb{C}^N$ represents the MISO downlink channel from the BS to user i; T is the transmission block length; $v_{i,t} \sim \mathcal{CN}(0, \sigma_v^2)$ is additive circular complex Gaussian noise.

Assuming perfect CSI at the BS, the task of SLP is to design the transmit signals $\{\boldsymbol{x}_t\}_{t=1}^T$ such that all the users receive their desired symbols with certain quality of service, which we will specify later. Let $\{s_{i,t}\}_{t=1}^T$ be the desired symbol stream for user i. We assume that $\{s_{i,t}\}_{t=1}^T$ is drawn from a QAM constellation

$$\mathcal{S}_i = \{s_R + \mathrm{j} s_I \mid s_R, s_I \in \{\pm 1, \pm 3, \ldots, \pm(2L_i - 1)\}\},$$

where L_i is a positive integer and the constellation size is $4L_i^2$. We seek to achieve

$$\boldsymbol{h}_i^H \boldsymbol{x}_t \approx d_i^R \Re(s_{i,t}) + \mathrm{j} d_i^I \Im(s_{i,t}), \quad \text{for all } i, t, \qquad (2)$$

where $\{d_i^R > 0\}_{i=1}^K$ and $\{d_i^I > 0\}_{i=1}^K$ represent the inter-point spacings of the received QAM constellations along the real and imaginary dimensions, respectively. See Fig. 1 for an illustration. The inter-point spacings are designed by the BS, and each user can acquire their corresponding inter-point spacings during the training phase. With knowledge of the inter-point spacings, the users detect their symbol streams by:

$$\hat{s}_{i,t} = \mathrm{dec}_i \left(\Re(y_{i,t})/d_i^R + \mathrm{j} \cdot \Im(y_{i,t})/d_i^I \right), \tag{3}$$

where dec_i denotes the decision function corresponding to $\mathcal{S}_i$.

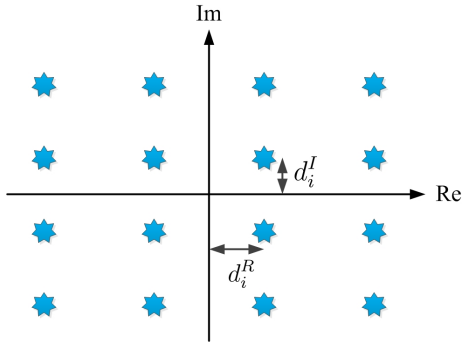

Fig. 1. Illustration of d_i^R and d_i^I for 16-QAM constellation

We are interested in an SEP-constrained SLP design formulation, where we seek to minimize the peak transmission energy among all the symbol times, and, at the same time, guarantee that the SEP of each user is no greater than a pre-specified value. The design is mathematically formulated as

$$\begin{aligned} \min_{\{\boldsymbol{x}_t\}_{t=1}^T, \boldsymbol{d}^R, \boldsymbol{d}^I} \ & \max_{t=1,\ldots,T} \ \|\boldsymbol{x}_t\|_2^2 \\ \text{s.t. } & \mathsf{SEP}_{i,t} \le \varepsilon_i, \quad i = 1,\ldots,K,\ t = 1,\ldots,T, \\ & \boldsymbol{d}^R \ge \boldsymbol{0}, \boldsymbol{d}^I \ge \boldsymbol{0}, \end{aligned} \tag{4}$$

where $\boldsymbol{d}^R = [\, d_1^R, \ldots, d_K^R \,]^T$, $\boldsymbol{d}^I = [\, d_1^I, \ldots, d_K^I \,]^T$, $\mathsf{SEP}_{i,t}$ denotes the symbol error probability of $s_{i,t}$ under (1)–(3), and ε_i's are pre-specified SEP requirements. Here, we optimize the inter-point spacings $\{\boldsymbol{d}^R, \boldsymbol{d}^I\}$ jointly with the transmit signals $\{\boldsymbol{x}_t\}_{t=1}^T$ for the whole transmission block. In other existing SLP works [13, 14] for QAM constellations, to some extent they prefix the inter-point spacings and consider optimizing the transmit signals on a per-symbol-time basis.

The next job is to characterize the SEP in the constraints of Problem (4). By standard SEP analysis and following similar derivations in our previous work [21], it can be shown that Problem (4) can be handled by the following problem

$$\begin{aligned} \min_{\{\boldsymbol{x}_t\}_{t=1}^T, \boldsymbol{d}^R, \boldsymbol{d}^I} \ & \max_{t=1,\ldots,T} \ \|\boldsymbol{x}_t\|_2^2 \\ \text{s.t. } & -\boldsymbol{d}^R + \boldsymbol{a}_t^R \le \Re(\boldsymbol{H}\boldsymbol{x}_t - \boldsymbol{d}^R \circ \boldsymbol{s}_t) \le \boldsymbol{d}^R - \boldsymbol{c}_t^R, \forall t, \\ & -\boldsymbol{d}^I + \boldsymbol{a}_t^I \le \Im(\boldsymbol{H}\boldsymbol{x}_t - \boldsymbol{d}^I \circ \boldsymbol{s}_t) \le \boldsymbol{d}^I - \boldsymbol{c}_t^I, \forall t, \\ & \boldsymbol{d}^R \ge \boldsymbol{0}, \boldsymbol{d}^I \ge \boldsymbol{0}. \end{aligned} \tag{5}$$

Here, $\circ$ denotes the element-wise product, $\boldsymbol{H} = [\, \boldsymbol{h}_1, \ldots, \boldsymbol{h}_K \,]^H$, $\boldsymbol{s}_t = [\, s_{1,t}, \ldots, s_{K,t} \,]^T$, $\boldsymbol{a}_t^R = [\, a_{1,t}^R, \ldots, a_{K,t}^R \,]^T$, $\boldsymbol{a}_t^I = [\, a_{1,t}^I, \ldots, a_{K,t}^I \,]^T$, $\boldsymbol{c}_t^R = [\, c_{1,t}^R, \ldots, c_{K,t}^R \,]^T$, $\boldsymbol{c}_t^I = [\, c_{1,t}^I, \ldots, c_{K,t}^I \,]^T$, where

$$a_{i,t}^R = \begin{cases} \alpha_i, & |\Re(s_{i,t})| < 2L_i - 1 \\ \beta_i, & \Re(s_{i,t}) = 2L_i - 1 \\ -\infty, & \Re(s_{i,t}) = -2L_i + 1 \end{cases}$$

$$c_{i,t}^R = \begin{cases} \alpha_i, & |\Re(s_{i,t})| < 2L_i - 1 \\ -\infty, & \Re(s_{i,t}) = 2L_i - 1 \\ \beta_i, & \Re(s_{i,t}) = -2L_i + 1 \end{cases}$$

with

$$\alpha_i = \frac{\sigma_v}{\sqrt{2}} Q^{-1}\left(\frac{1 - \sqrt{1-\varepsilon_i}}{2} \right), \quad \beta_i = \frac{\sigma_v}{\sqrt{2}} Q^{-1}\left(1 - \sqrt{1-\varepsilon_i} \right),$$

and the same result applies to $a_{i,t}^I$ and $c_{i,t}^I$ if we replace "$\Re$" with "$\Im$". By complex-to-real transformation, Problem (5) can be equivalently expressed as

$$\begin{aligned} \min_{\{\bar{\boldsymbol{x}}_t \in \mathbb{R}^{2N}\}_{t=1}^T, \bar{\boldsymbol{d}} \in \mathbb{R}^{2K}} \ & \max_{t=1,\ldots,T} \ \|\bar{\boldsymbol{x}}_t\|_2^2 \\ \text{s.t. } & -\bar{\boldsymbol{d}} + \bar{\boldsymbol{a}}_t \le \bar{\boldsymbol{H}}\bar{\boldsymbol{x}}_t - \bar{\boldsymbol{d}} \circ \bar{\boldsymbol{s}}_t \le \bar{\boldsymbol{d}} - \bar{\boldsymbol{c}}_t, \forall t, \\ & \bar{\boldsymbol{d}} \ge \boldsymbol{0}, \end{aligned} \tag{6}$$

where

$$\bar{\boldsymbol{H}} = \begin{bmatrix} \Re(\boldsymbol{H}) & -\Im(\boldsymbol{H}) \\ \Im(\boldsymbol{H}) & \Re(\boldsymbol{H}) \end{bmatrix}, \ \bar{\boldsymbol{d}} = \begin{bmatrix} \boldsymbol{d}^R \\ \boldsymbol{d}^I \end{bmatrix}, \ \bar{\boldsymbol{x}}_t = \begin{bmatrix} \Re(\boldsymbol{x}_t) \\ \Im(\boldsymbol{x}_t) \end{bmatrix}, \tag{7}$$

$$\bar{\boldsymbol{a}}_t = \begin{bmatrix} \boldsymbol{a}_t^R \\ \boldsymbol{a}_t^I \end{bmatrix}, \ \bar{\boldsymbol{c}}_t = \begin{bmatrix} \boldsymbol{c}_t^R \\ \boldsymbol{c}_t^I \end{bmatrix}, \ \bar{\boldsymbol{s}}_t = \begin{bmatrix} \Re(\boldsymbol{s}_t) \\ \Im(\boldsymbol{s}_t) \end{bmatrix}. \tag{8}$$

Problem (6) can be reformulated as a symbol-perturbed ZF form by the result in [21], which is shown as follows.

Proposition 1 *Suppose that $\bar{\boldsymbol{H}}$ has full row rank. The optimal solution $\bar{\boldsymbol{x}}_t^\star$'s to Problem* (6) *is given by*

$$\bar{\boldsymbol{x}}_t^\star = \bar{\boldsymbol{H}}^\dagger (\bar{\boldsymbol{d}}^\star \circ \bar{\boldsymbol{s}}_t + \bar{\boldsymbol{u}}_t^\star), \quad t = 1,\ldots,T,$$

where $\bar{\boldsymbol{H}}^\dagger = \bar{\boldsymbol{H}}^T(\bar{\boldsymbol{H}}\bar{\boldsymbol{H}}^T)^{-1}$ is the pseudo-inverse of $\bar{\boldsymbol{H}}$, and $\bar{\boldsymbol{u}}_1^\star, \ldots, \bar{\boldsymbol{u}}_T^\star, \bar{\boldsymbol{d}}^\star$ is the optimal solution to

$$\begin{aligned} \min_{\{\bar{\boldsymbol{u}}_t\}_{t=1}^T, \bar{\boldsymbol{d}}} \ & \max_{t=1,\ldots,T} \ (\bar{\boldsymbol{d}} \circ \bar{\boldsymbol{s}}_t + \bar{\boldsymbol{u}}_t)^T \bar{\boldsymbol{R}} (\bar{\boldsymbol{d}} \circ \bar{\boldsymbol{s}}_t + \bar{\boldsymbol{u}}_t) \\ \text{s.t. } & -\bar{\boldsymbol{d}} + \bar{\boldsymbol{a}}_t \le \bar{\boldsymbol{u}}_t \le \bar{\boldsymbol{d}} - \bar{\boldsymbol{c}}_t, \forall t, \\ & \bar{\boldsymbol{d}} \ge \boldsymbol{0}, \end{aligned} \tag{9}$$

with $\bar{\boldsymbol{R}} = (\bar{\boldsymbol{H}}\bar{\boldsymbol{H}}^T)^{-1}$.

The advantage of the reformulation in (9) is that the constraints of Problem (9) are simple bound constraints, which are easier to handle than those of Problem (6). Also, it should be noted that Problem (9) (and also Problem (6)) is convex.

3. PROPOSED ALGORITHM

In this section we develop a fast algorithm for the SEP-constrained SLP design in (9). First, we should mention that the transmission block length T is often large in practice, say, a few hundreds. Thus, Problem (9) is a large-scale problem. If we call general-purpose solvers, such as CVX, to solve Problem (9), it will take a long time to complete the process. This motivates us to study how the problem structure can be utilized to build a fast algorithm for Problem (9).

3.1. Smooth Approximation and ADMM Algorithm

Our idea is to use ADMM to decouple the problem into per-symbol-time subproblems. To do it, we first apply the log-sum-exponential (LSE) approximation to the objective function of Problem (9), which gives

$$\begin{aligned}\min_{\{\bar{\boldsymbol{u}}_t\}_{t=1}^T,\bar{\boldsymbol{d}}} \ & \tfrac{1}{\beta}\log\left(\textstyle\sum_{t=1}^T e^{\beta(\bar{\boldsymbol{d}}\circ\bar{\boldsymbol{s}}_t+\bar{\boldsymbol{u}}_t)^T\bar{\boldsymbol{R}}(\bar{\boldsymbol{d}}\circ\bar{\boldsymbol{s}}_t+\bar{\boldsymbol{u}}_t)}\right)\\ \text{s.t.} \ & -\bar{\boldsymbol{d}}+\bar{\boldsymbol{a}}_t\le\bar{\boldsymbol{u}}_t\le\bar{\boldsymbol{d}}-\bar{\boldsymbol{c}}_t,\quad t=1,\dots,T,\\ & \bar{\boldsymbol{d}}\ge\boldsymbol{0},\end{aligned} \tag{10}$$

where β is the smoothing parameter of the LSE approximation (the approximation error vanishes as $\beta\to\infty$). Observe that it makes no difference for the optimal solution of (10) if we remove log and $1/\beta$ from the objective function. In order to apply ADMM, we split the variable $\bar{\boldsymbol{d}}$ into $\bar{\boldsymbol{d}}_1=\ldots=\bar{\boldsymbol{d}}_T=\bar{\boldsymbol{d}}$; i.e., we rewrite Problem (10) as

$$\begin{aligned}\min_{\{\bar{\boldsymbol{u}}_t,\bar{\boldsymbol{d}}_t\}_{t=1}^T,\bar{\boldsymbol{d}}} \ & \textstyle\sum_{t=1}^T e^{\beta(\bar{\boldsymbol{d}}_t\circ\bar{\boldsymbol{s}}_t+\bar{\boldsymbol{u}}_t)^T\bar{\boldsymbol{R}}(\bar{\boldsymbol{d}}_t\circ\bar{\boldsymbol{s}}_t+\bar{\boldsymbol{u}}_t)}\\ \text{s.t.} \ & -\bar{\boldsymbol{d}}_t+\bar{\boldsymbol{a}}_t\le\bar{\boldsymbol{u}}_t\le\bar{\boldsymbol{d}}_t-\bar{\boldsymbol{c}}_t,\quad t=1,\dots,T,\\ & \bar{\boldsymbol{d}}_t\ge\boldsymbol{0},\quad t=1,\dots,T,\\ & \bar{\boldsymbol{d}}_1=\bar{\boldsymbol{d}}_2=\cdots=\bar{\boldsymbol{d}}_T=\bar{\boldsymbol{d}}.\end{aligned} \tag{11}$$

For ease of exposition, we reformulate the above problem as

$$\begin{aligned}\min_{\{\bar{\boldsymbol{u}}_t,\bar{\boldsymbol{d}}_t\}_{t=1}^T,\bar{\boldsymbol{d}}} \ & \textstyle\sum_{t=1}^T\left\{e^{\beta(\bar{\boldsymbol{d}}_t\circ\bar{\boldsymbol{s}}_t+\bar{\boldsymbol{u}}_t)^T\bar{\boldsymbol{R}}(\bar{\boldsymbol{d}}_t\circ\bar{\boldsymbol{s}}_t+\bar{\boldsymbol{u}}_t)}+\mathcal{I}_{\mathcal{C}_t}(\bar{\boldsymbol{u}}_t,\bar{\boldsymbol{d}}_t)\right\}\\ \text{s.t.} \ & \bar{\boldsymbol{d}}_t=\bar{\boldsymbol{d}},\quad t=1,\dots,T,\end{aligned} \tag{12}$$

where

$$\mathcal{C}_t\triangleq\{(\bar{\boldsymbol{u}}_t,\bar{\boldsymbol{d}}_t)\mid -\bar{\boldsymbol{d}}_t+\bar{\boldsymbol{a}}_t\le\bar{\boldsymbol{u}}_t\le\bar{\boldsymbol{d}}_t-\bar{\boldsymbol{c}}_t,\bar{\boldsymbol{d}}_t\ge\boldsymbol{0}\},$$

and $\mathcal{I}_{\mathcal{C}_t}(\bar{\boldsymbol{u}}_t,\bar{\boldsymbol{d}}_t)$ denotes the indicator function of $\mathcal{C}_t$, i.e.,

$$\mathcal{I}_{\mathcal{C}_t}(\bar{\boldsymbol{u}}_t,\bar{\boldsymbol{d}}_t)=\begin{cases}0, & \text{if } (\bar{\boldsymbol{u}}_t,\bar{\boldsymbol{d}}_t)\in\mathcal{C}_t\\ +\infty, & \text{if } (\bar{\boldsymbol{u}}_t,\bar{\boldsymbol{d}}_t)\notin\mathcal{C}_t\end{cases} \tag{13}$$

The augmented Lagrangian function of Problem (12) is defined as

$$\begin{aligned}\mathcal{L}_\rho(\bar{\boldsymbol{U}},\bar{\boldsymbol{D}},\bar{\boldsymbol{d}},\boldsymbol{\Lambda})=\sum_{t=1}^T\{\ & e^{\beta(\bar{\boldsymbol{d}}_t\circ\bar{\boldsymbol{s}}_t+\bar{\boldsymbol{u}}_t)^T\bar{\boldsymbol{R}}(\bar{\boldsymbol{d}}_t\circ\bar{\boldsymbol{s}}_t+\bar{\boldsymbol{u}}_t)}+\mathcal{I}_{\mathcal{C}_t}(\bar{\boldsymbol{u}}_t,\bar{\boldsymbol{d}}_t)\\ & -\langle\boldsymbol{\lambda}_t,\bar{\boldsymbol{d}}-\bar{\boldsymbol{d}}_t\rangle+\frac{\rho}{2}\|\bar{\boldsymbol{d}}-\bar{\boldsymbol{d}}_t\|_2^2\ \},\end{aligned}$$

where $\bar{\boldsymbol{U}}=[\bar{\boldsymbol{u}}_1,\dots,\bar{\boldsymbol{u}}_T]$, $\bar{\boldsymbol{D}}=[\bar{\boldsymbol{d}}_1,\dots,\bar{\boldsymbol{d}}_T]$, $\rho>0$, and $\boldsymbol{\Lambda}=[\boldsymbol{\lambda}_1,\dots,\boldsymbol{\lambda}_T]$ denotes the dual variables. In accordance with the ADMM literature [22], the ADMM iterations are

$$(\bar{\boldsymbol{U}}^{(k)},\bar{\boldsymbol{D}}^{(k)})=\arg\min_{\bar{\boldsymbol{U}},\bar{\boldsymbol{D}}}\mathcal{L}_\rho(\bar{\boldsymbol{U}},\bar{\boldsymbol{D}},\bar{\boldsymbol{d}}^{(k-1)},\boldsymbol{\Lambda}^{(k-1)}), \tag{14}$$

$$\bar{\boldsymbol{d}}^{(k)}=\arg\min_{\bar{\boldsymbol{d}}}\mathcal{L}_\rho(\bar{\boldsymbol{U}}^{(k)},\bar{\boldsymbol{D}}^{(k)},\bar{\boldsymbol{d}},\boldsymbol{\Lambda}^{(k-1)}), \tag{15}$$

$$\boldsymbol{\lambda}_t^{(k)}=\boldsymbol{\lambda}_t^{(k-1)}-\rho(\bar{\boldsymbol{d}}^{(k)}-\bar{\boldsymbol{d}}_t^{(k)}),\quad t=1,\dots,T. \tag{16}$$

3.2. Algorithms for the ADMM-Decoupled Problems

Our remaining task is to derive efficient solutions to the ADMM-decoupled problems in (14)–(15). For Problem (15), the update of $\bar{\boldsymbol{d}}^{(k)}$ admits a closed-form solution

$$\bar{\boldsymbol{d}}^{(k)}=\frac{1}{\rho T}\sum_{t=1}^T(\rho\bar{\boldsymbol{d}}_t^{(k)}+\boldsymbol{\lambda}_t^{(k-1)}). \tag{17}$$

For Problem (14), it can be decoupled as per-symbol-time problems

$$\begin{aligned}\min_{\bar{\boldsymbol{u}}_t,\bar{\boldsymbol{d}}_t} \ & f(\bar{\boldsymbol{u}}_t,\bar{\boldsymbol{d}}_t)\\ \text{s.t.} \ & -\bar{\boldsymbol{d}}_t+\bar{\boldsymbol{a}}_t\le\bar{\boldsymbol{u}}_t\le\bar{\boldsymbol{d}}_t-\bar{\boldsymbol{c}}_t,\\ & \bar{\boldsymbol{d}}_t\ge\boldsymbol{0},\end{aligned} \tag{18}$$

for $t=1,\dots,T$, where

$$\begin{aligned}f(\bar{\boldsymbol{u}}_t,\bar{\boldsymbol{d}}_t)\triangleq\ & e^{\beta(\bar{\boldsymbol{d}}_t\circ\bar{\boldsymbol{s}}_t+\bar{\boldsymbol{u}}_t)^T\bar{\boldsymbol{R}}(\bar{\boldsymbol{d}}_t\circ\bar{\boldsymbol{s}}_t+\bar{\boldsymbol{u}}_t)}-\langle\boldsymbol{\lambda}_t,\bar{\boldsymbol{d}}^{(k-1)}-\bar{\boldsymbol{d}}_t\rangle\\ & +\frac{\rho}{2}\|\bar{\boldsymbol{d}}^{(k-1)}-\bar{\boldsymbol{d}}_t\|_2^2.\end{aligned}$$

The problems in (18) do not admit closed-form solutions in general, but we can custom-derive a fast algorithm for them. Specifically, we employ the accelerated proximal gradient (APG) method [23]. Let $\bar{\boldsymbol{z}}_t=(\bar{\boldsymbol{u}}_t,\bar{\boldsymbol{d}}_t)$ for convenience. The APG iterations for (18) are given by

$$\boldsymbol{v}^{(k)}=\Pi_{\mathcal{C}_t}\left(\bar{\boldsymbol{z}}_t^{(k)}-\eta_k\nabla f(\bar{\boldsymbol{z}}_t^{(k)})\right), \tag{19}$$

$$\bar{\boldsymbol{z}}_t^{(k+1)}=\boldsymbol{v}^{(k)}+\frac{t_k-1}{t_{k+1}}\left(\boldsymbol{v}^{(k)}-\boldsymbol{v}^{(k-1)}\right), \tag{20}$$

where $t_{k+1}=\frac{1+\sqrt{1+4t_k^2}}{2}$; η_k is the step size at iteration k and is determined by backtracking line search; $\Pi_{\mathcal{X}}(\boldsymbol{x})\triangleq\arg\min_{\boldsymbol{y}\in\mathcal{X}}\|\boldsymbol{x}-\boldsymbol{y}\|_2^2$ is defined as the projection of $\boldsymbol{x}$ onto $\mathcal{X}$.

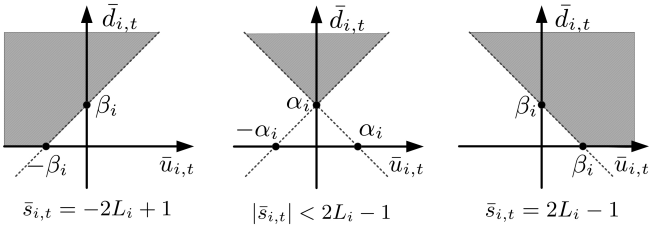

Fig. 2. Constraint of $(\bar{u}_{i,t},\bar{d}_{i,t})$ for all possible choices of $\bar{s}_{i,t}$.

As a key component for the APG method, we need to find an efficient way to compute the projection $\Pi_{\mathcal{C}_t}$. As it turns out, the projection $\Pi_{\mathcal{C}_t}$ is very easy to compute. To describe, let $(\tilde{\boldsymbol{u}}_t,\tilde{\boldsymbol{d}}_t)=\Pi_{\mathcal{C}_t}(\hat{\boldsymbol{u}}_t,\hat{\boldsymbol{d}}_t)$. It can be shown that for $|\bar{s}_{i,t}|<2L_i-1$,

$$(\tilde{u}_{i,t},\tilde{d}_{i,t})=\begin{cases}(0,\alpha_i), & \text{for } |\hat{u}_{i,t}|\le\alpha_i-\hat{d}_{i,t},\\ (\hat{u}_{i,t}-\delta_1,\hat{d}_{i,t}+\delta_1), & \text{for } |\hat{d}_{i,t}-\alpha_i|\le\hat{u}_{i,t},\\ (\hat{u}_{i,t}+\delta_2,\hat{d}_{i,t}+\delta_2), & \text{for } |\hat{d}_{i,t}-\alpha_i|\le-\hat{u}_{i,t},\\ (\hat{u}_{i,t},\hat{d}_{i,t}), & \text{otherwise,}\end{cases}$$

where $\delta_1=|\hat{d}_{i,t}-\hat{u}_{i,t}-\alpha_i|/2$ and $\delta_2=|\hat{d}_{i,t}+\hat{u}_{i,t}-\alpha_i|/2$; and that for $|\bar{s}_{i,t}|=2L_i-1$,

$$(\tilde{u}_{i,t},\tilde{d}_{i,t})=\begin{cases}(\kappa\max\{\beta_i,\kappa\hat{u}_{i,t}\},0), & \text{for } \hat{d}_{i,t}\le 0,\\ (\hat{u}_{i,t}+\kappa\delta,\hat{d}_{i,t}+\delta), & \text{for } \kappa\hat{u}_{i,t}+\hat{d}_{i,t}\le\beta_i,\\ & \ \ \&\ \hat{d}_{i,t}\ge 0,\\ (\hat{u}_{i,t},\hat{d}_{i,t}), & \text{otherwise,}\end{cases}$$

where $\kappa = \text{sign}(\bar{s}_{i,t})$ and $\delta = |\hat{d}_{i,t} + \kappa\hat{u}_{i,t} - \beta_i|/2$. The idea that leads to the above solution is to observe the constraint set under different cases of $\bar{\boldsymbol{s}}_t$; see Fig. 2.

4. SIMULATION RESULTS

In this section, we evaluate the performance of our proposed algorithm by Monte-Carlo simulations. In the simulation, we consider the peak transmission energy $\max_{t=1,\ldots,T} \|\boldsymbol{x}_t\|_2^2$ as the performance metric.

Also, to provide benchmarking for our proposed algorithm, we consider two traditional linear precoding schemes: ZF and the optimal linear beamforming (OLB). They are designed such that the SEP requirements are satisfied; see [21] for details. We should note that both are unable to perform minimization of the peak transmission energy since they are not symbol-level precoding techniques.

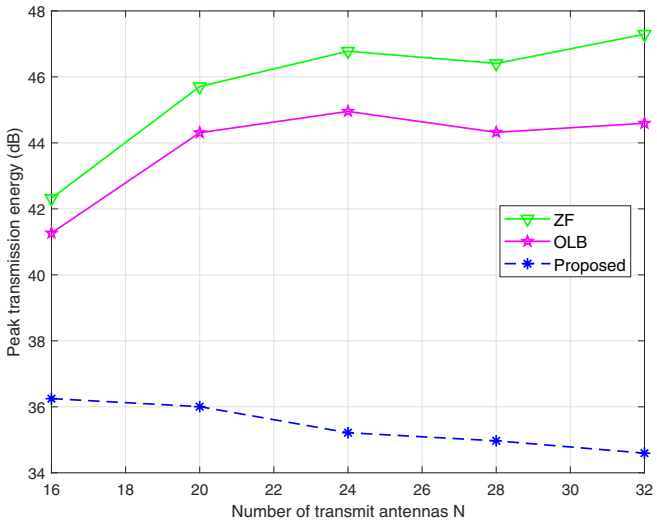

Fig. 3. Peak transmission energy w.r.t. N; $K = N$.

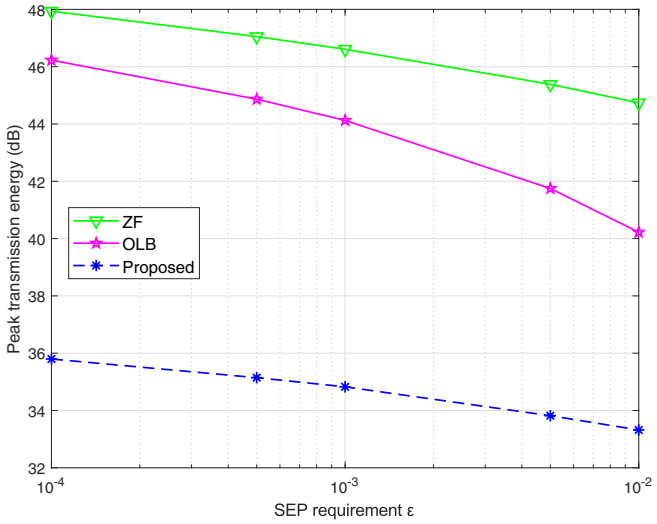

Fig. 4. Peak transmission energy w.r.t. ε; $N = 32$, $K = 32$.

The simulation settings are as follows. The power of noise is $\sigma_v^2 = 1$; the transmission block length is $T = 200$; the channels are block Rayleigh fading channels, which means that the elements h_{ij} of $\boldsymbol{H}$ follow $\mathcal{CN}(0,1)$ in an i.i.d. manner; the symbols $s_{i,t}$'s are drawn uniformly from 16-QAM constellation; we set $\varepsilon_1 = \cdots = \varepsilon_K = \varepsilon$. The results to be shown are averages over 100 channel realizations. We should also specify the settings of our proposed algorithm. The penalty parameter is $\rho = 100$; the smoothing parameter $\beta = 0.001$; we initialize $\bar{\boldsymbol{d}}^{(0)} = [\boldsymbol{\alpha}; \boldsymbol{\alpha}]$ with $\boldsymbol{\alpha} = [\alpha_1, \ldots, \alpha_K]^T$, and $\boldsymbol{\Lambda}^{(0)} = \boldsymbol{0}$.

Fig. 3 shows the peak transmission energy for different number of transmit antennas. In this simulation scenario, we set $K = N$. In the legend, "ZF" represents the zero-forcing beamforming scheme; "OLB" stands for the optimal linear beamforming scheme; "Proposed" means our proposed ADMM algorithm for the SEP-constrained SLP design. We see from the figure that there is a large performance gap between our proposed algorithm and the benchmarked schemes, and the gap tends to increase with larger N and K.

Fig. 4 compares the peak transmission energy performance of all the considered precoding schemes when $N = K = 32$. We evaluate the performance for different SEP requirements ε. We see that our proposed SLP design significantly outperforms ZF and OLB in terms of peak transmission energy. In particular, the performance gain is about 10dB at the SEP level $\varepsilon = 10^{-4}$.

5. CONCLUSIONS

To conclude, in this work we tackled an SEP-constrained SLP design formulation for peak transmission energy minimization under general QAM constellations. We devised an ADMM algorithm to solve the design problem, which is of large scale. Simulation results show that our proposed algorithm can achieve much better performance than some existing linear precoding schemes.

6. REFERENCES

[1] M. Bengtsson and B. Ottersten, "Optimal and suboptimal transmit beamforming," Chapter 18 in *Handbook of Antennas in Wireless Communications*, L. C. Godara, Ed., CRC Press, Aug. 2001.

[2] M. Schubert and H. Boche, "Solution of the multiuser downlink beamforming problem with individual SINR constraints," *IEEE Trans. Veh. Technol.*, vol. 53, no. 1, pp. 18–28, 2004.

[3] A. Wiesel, Y. C. Eldar, and S. Shamai, "Linear precoding via conic optimization for fixed MIMO receivers," *IEEE Trans. Signal Process.*, vol. 54, no. 1, pp. 161–176, 2006.

[4] ——, "Zero-forcing precoding and generalized inverses," *IEEE Trans. Signal Process.*, vol. 56, no. 9, pp. 4409–4418, 2008.

[5] A. B. Gershman, N. D. Sidiropoulos, S. Shahbazpanahi, M. Bengtsson, and B. Ottersten, "Convex optimization-based beamforming," *IEEE Signal Process. Mag.*, vol. 27, no. 3, pp. 62–75, 2010.

[6] Q. Shi, M. Razaviyayn, Z.-Q. Luo, and C. He, "An iteratively weighted MMSE approach to distributed sum-utility maximization for a MIMO interfering broadcast channel," *IEEE Trans. Signal Process.*, vol. 59, no. 9, pp. 4331–4340, 2011.

[7] C. Masouros and E. Alsusa, "A novel transmitter-based selective-precoding technique for DS/CDMA systems," *IEEE Signal Process. Lett.*, vol. 14, no. 9, pp. 637–640, 2007.

[8] ——, "Dynamic linear precoding for the exploitation of known interference in MIMO broadcast systems," *IEEE Trans. Wireless Commun.*, vol. 8, no. 3, pp. 1396–1404, 2009.

[9] C. Masouros, "Correlation rotation linear precoding for MIMO broadcast communications," *IEEE Trans. Signal Process.*, vol. 59, no. 1, pp. 252–262, 2011.

[10] C. Masouros and G. Zheng, "Exploiting known interference as green signal power for downlink beamforming optimization," *IEEE Trans. Signal Process.*, vol. 63, no. 14, pp. 3628–3640, 2015.

[11] M. Alodeh, S. Chatzinotas, and B. Ottersten, "Constructive multiuser interference in symbol level precoding for the MISO downlink channel," *IEEE Trans. Signal process.*, vol. 63, no. 9, pp. 2239–2252, 2015.

[12] A. Kalantari, M. Soltanalian, S. Maleki, S. Chatzinotas, and B. Ottersten, "Directional modulation via symbol-level precoding: A way to enhance security," *IEEE J. Sel. Topics Signal Process.*, vol. 10, no. 8, pp. 1478–1493, 2016.

[13] A. Kalantari, C. Tsinos, M. Soltanalian, S. Chatzinotas, W.-K. Ma, and B. Ottersten, "MIMO directional modulation M-QAM precoding for transceivers performance enhancement," in *Proc. 2017 IEEE 18th International Workshop on Signal Processing Advances in Wireless Communications (SPAWC)*.

[14] M. Alodeh, S. Chatzinotas, and B. Ottersten, "Symbol-level multiuser MISO precoding for multi-level adaptive modulation," *IEEE Trans. Wireless Commun.*, vol. 16, no. 8, pp. 5511–5524, 2017.

[15] M. Alodeh, D. Spano, A. Kalantari, C. Tsinos, D. Christopoulos, S. Chatzinotas, and B. Ottersten, "Symbol-level and multicast precoding for multiuser multiantenna downlink: A state-of-the-art, classification and challenges," *IEEE Commun. Surveys Tuts.*, 2018.

[16] D. Spano, M. Alodeh, S. Chatzinotas, and B. Ottersten, "Symbol-level precoding for the nonlinear multiuser MISO downlink channel," *IEEE Trans. Signal Process.*, vol. 66, no. 5, pp. 1331–1345, 2018.

[17] M. R. Khandaker, C. Masouros, and K.-K. Wong, "Constructive interference based secure precoding: A new dimension in physical layer security," *IEEE Trans. Inf. Forensics Security*, vol. 13, no. 9, pp. 2256–2268, 2018.

[18] P. V. Amadori and C. Masouros, "Large scale antenna selection and precoding for interference exploitation," *IEEE Trans. Commun.*, vol. 65, no. 10, pp. 4529–4542, 2017.

[19] M. T. Kabir, M. R. Khandaker, and C. Masouros, "Robust energy harvesting FD transmission: Interference suppression vs exploitation," *IEEE Commun. Lett.*, vol. 22, no. 9, pp. 1866–1869, 2018.

[20] A. Haqiqatnejad, F. Kayhan, and B. Ottersten, "Robust design of power minimizing symbol-level precoder under channel uncertainty," *arXiv preprint arXiv:1805.02395*, 2018.

[21] Y. Liu and W.-K. Ma, "Symbol-level precoding is symbol-perturbed ZF when energy efficiency is sought," in *Proc. 2018 IEEE International Conference on Acoustics, Speech and Signal Processing (ICASSP)*, 2018, pp. 3869–3873.

[22] S. Boyd, N. Parikh, E. Chu, B. Peleato, J. Eckstein *et al.*, "Distributed optimization and statistical learning via the alternating direction method of multipliers," *Foundations and Trends ® in Machine learning*, vol. 3, no. 1, pp. 1–122, 2011.

[23] A. Beck and M. Teboulle, "A fast iterative shrinkage-thresholding algorithm for linear inverse problems," *SIAM journal on imaging sciences*, vol. 2, no. 1, pp. 183–202, 2009.